

## A Mössbauer spectral study of the $\text{GdCo}_{4-x}\text{Fe}_x\text{B}$ compounds

Fernande Grandjean, Raphaël P. Hermann, E. Popiel, and Gary J. Long

Citation: *Journal of Applied Physics* **101**, 023917 (2007);

View online: <https://doi.org/10.1063/1.2400115>

View Table of Contents: <http://aip.scitation.org/toc/jap/101/2>

Published by the *American Institute of Physics*

---

---



# SciLight

Sharp, quick summaries **illuminating**  
the latest physics research

Sign up for **FREE!**

AIP  
Publishing

# A Mössbauer spectral study of the $\text{GdCo}_{4-x}\text{Fe}_x\text{B}$ compounds

Fernande Grandjean<sup>a)</sup> and Raphaël P. Hermann<sup>b)</sup>

*Department of Physics, B5, University of Liège, B-4000 Sart-Tilman, Belgium*

E. Popiel

*Institute of Physics, Silesian University, PL-40007 Katowice, Poland*

Gary J. Long<sup>c)</sup>

*Department of Chemistry, University of Missouri-Rolla, Rolla, Montana 65409-0010*

(Received 26 July 2006; accepted 28 September 2006; published online 30 January 2007)

The iron-57 Mössbauer spectra of the  $\text{GdCo}_{4-x}\text{Fe}_x\text{B}$  compounds, where  $x$  is 0.10, 0.15, 0.20, 0.25, 1, 2, 2.5, and 2.6, have been measured at room temperature and reveal relatively small iron hyperfine fields of approximately 12–18 T, relatively large quadrupole interactions of approximately +0.9 and –1 mm/s, and three very different types of spectra for  $x=0.10$  and 0.15,  $x=0.25$ , 1, and 2, and  $x=2.5$  and 2.6. The differences result from both the different easy magnetization directions in these compounds and the different cobalt and/or iron occupancies of the crystallographic 2c and 6i sites. The spectra have been fitted by calculating the spectral absorption with the complete iron-57 nuclear excited state Hamiltonian for the iron 2c and 6i sites. The fits have used an asymmetry parameter  $\eta$  and Euler angles  $\theta$  and  $\phi$  that relate the hyperfine field to the iron electric field gradient axes of each crystallographic site in an orientation that is consistent with the structural and magnetic properties of the site. The results of the fits indicate both that the full Hamiltonian approach is required for physically reasonable spectral fits and that the small observed fields result from the presence of large orbital contributions which subtract from the Fermi contact contributions to the magnetic hyperfine fields of the two sites. The iron 2c occupancy obtained from the Mössbauer spectral area has been used to model the compositional dependence of the magnetic anisotropy constant in the  $\text{GdCo}_{4-x}\text{Fe}_x\text{B}$  compounds. © 2007 American Institute of Physics.  
[DOI: 10.1063/1.2400115]

## I. INTRODUCTION

The initial work<sup>1</sup> of Kuz'ma and Bilonizhko in 1974 has led to the preparation and study<sup>2–12</sup> of a variety of  $\text{RCo}_{4-x}\text{Fe}_x\text{B}$  compounds in which  $R$  is yttrium or different rare earths and in which  $x$  can range in some cases from 0 to 4. These compounds are of interest because they can exhibit either axial or basal magnetic anisotropy that can change as a function of rare earth, composition, and/or temperature. Furthermore, the  $\text{RCo}_{4-x}\text{Fe}_x\text{B}$  structures are of special interest because they are closely related to those of the  $\text{RCO}_5$  compounds, which are extensively used as hard permanent magnets. Indeed, the structure of the  $\text{RCo}_{4-x}\text{Fe}_x\text{B}$  compounds may be obtained from that of the  $\text{RCO}_5$  compounds by replacing one cobalt with one boron. Some of the  $\text{RCo}_{4-x}\text{Fe}_x\text{B}$  compounds also appear in the rare earth, iron, and boron ternary phase diagrams phase diagrams that also contain the  $\text{R}_2\text{Fe}_{14}\text{B}$  hard magnetic compounds. Finally, the  $\text{RCo}_{4-x}\text{Fe}_x\text{B}$  compounds, where  $R$  is a heavy rare earth, are useful for magneto-optical applications because they show a compensation point whose temperature can be adjusted by controlling the rare-earth and transition metal compositions. Thus, it is important to understand both the macroscopic and microscopic properties of the  $\text{RCo}_{4-x}\text{Fe}_x\text{B}$  compounds.

Here, the Mössbauer spectra of the  $\text{GdCo}_{4-x}\text{Fe}_x\text{B}$  compounds, with  $x=0.10$ , 0.15, 0.20, 0.25, 1, 2, 2.5, and 2.6, spectra that have been reported<sup>7</sup> earlier, are analyzed in full detail and provide an insight about the magnetism of the iron sublattices.

## II. EXPERIMENT

The samples of  $\text{GdCo}_{4-x}\text{Fe}_x\text{B}$ , with  $0.10 \leq x \leq 2.6$  used here are the same as those prepared and characterized earlier.<sup>7</sup> The Mössbauer spectra have been measured at room temperature on a constant-acceleration spectrometer which utilized a chromium matrix cobalt-57 source and was calibrated at room temperature with  $\alpha$ -iron powder. The statistical errors associated with all the fitted parameters are given in Table I. The actual errors are probably twice as large as the statistical errors.

## III. MÖSSBAUER SPECTRAL ANALYSIS

The room temperature Mössbauer spectra of the  $\text{GdCo}_{4-x}\text{Fe}_x\text{B}$  compounds, with  $0.10 \leq x \leq 0.25$  and with  $1 \leq x \leq 2.6$ , are shown in Figs. 1 and 2, respectively. An initial inspection of these spectra reveals several interesting results. First, the iron hyperfine fields are relatively small at approximately 12–18 T, which are in approximate agreement with the small 3d moments of  $(0.8\text{--}1.5)\mu_B$  that have been reported<sup>7</sup> earlier for these compounds. Second, the spectra may be divided into three groups with very different spectral

<sup>a)</sup>Electronic mail: fgrandjean@ulg.ac.be

<sup>b)</sup>Present address: Institut für Festkörperforschung, Forschungszentrum Jülich GmbH, D-52425 Jülich, Germany.

<sup>c)</sup>Electronic mail: glong@umr.edu

TABLE I. Room temperature Mössbauer spectral parameters of the  $\text{GdCo}_{4-x}\text{Fe}_x\text{B}$  compounds. The parameters are defined in the text and given with statistical error limits if they have been refined.

$x$	Site	$\delta^a$ (mm/s)	$e^2Qq/2$ (mm/s)	$H$ (T)	$\eta$	$\theta$ (deg)	$\phi$ , (deg)	% area	$\Gamma$ (mm/s)	$\Delta\Gamma$	$y$
0.10	$2c_{\parallel}$	0.006(3)	-1.028(6)	13.73(1)	0	0	...	93.5(6)	0.22(1)	0	1.12
	imp <sup>b</sup>	0.25	0.26	0	...	...	...	6.5(6)	0.27(7)	0	1.12
0.15	$2c_{\parallel}$	-0.003(3)	-1.0(1)	13.77(2)	0	0	...	66(1)	0.30(1)	0	1.56
	$2c_{\perp}$	-0.003(3)	-1.01(1)	12.2(1)	0	90	0	14(2)	0.35(5)	0	1.56
	imp <sup>b</sup>	0.25	0.26	0	...	...	...	20(1)	0.31(2)	0	1.56
0.20	$2c_{\parallel}$	-0.011(1)	-0.907(6)	13.79(3)	0	0	...	37.4(5)	0.450(4)	0.004(2)	1.45
	$2c_{\perp}$	-0.011(1)	-0.907(6)	12.39(2)	0	90	0	54.4(5)	0.240(1)	0.010(1)	1.45
	imp <sup>b</sup>	0.25	0.26	0	...	...	...	8.2(2)	0.26(2)	0	1.45
0.25	$2c_{\perp}$	-0.005(2)	-0.97(1)	12.30(2)	0	90	0	100	0.22(1)	0.029(5)	1.38
0.25 <sup>c</sup>	$2c_{\perp}$	-0.006(2)	-0.96(1)	12.23(5)	0	90	0	100	0.219(2)	0	1.29
1.0	$2c_{\parallel}$	0.002(1)	-0.895(6)	13.65(1)	0	90	0	72.0(6)	0.247(6)	0.061(3)	2
	$6i_1$	0.006(6)	0.89(1)	12.6(1)	1	0	90	9.4(6)	0.247(6)	0.13(1)	2
	$6i_2$	-0.006(6)	0.89(1)	12.08(5)	1	120	90	18.6(6)	0.247(6)	0.13(1)	2
2.0	$2c_{\perp}$	-0.013(2)	-0.85(1)	15.50(2)	0	90	0	43	0.232(6)	0.074(4)	3.51
	$6i^c$	0.03	0.75(1)	13.6(8)	1	0	90	38	0.44(1)	0	3.51
	$6i_2^c$	0.03	0.75(1)	13.4(2)	1	120	90	19	0.44(1)	0	3.51
2.5 <sup>c</sup>	$2c_{\parallel}$	0.06(1)	-0.85(1)	18.1(1)	0	0	...	29.4	0.293(4)	0	2.00
	$6i$	0.04(1)	0.78(1)	14.65(6)	1	90	0	70.6	0.293(4)	0	2.00
2.6 <sup>c</sup>	$2c_{\parallel}$	0.04(1)	-0.85(1)	18.31(5)	0	0	...	29.4	0.263(3)	0	1.96
	$6i$	0.04(1)	0.78(1)	14.72(3)	1	90	0	70.6	0.263(3)	0	1.96

<sup>a</sup>The isomer shifts are given relative to room temperature  $\alpha$ -iron foil.

<sup>b</sup>Hyperfine parameters constrained to those expected for traces of iron in beryllium.

<sup>c</sup>The weighted average parameters obtained from the binomial distribution fits.

profiles, the first with  $x=0.10$  and  $0.15$ , the second with  $x=0.25$ ,  $1$ , and  $2$ , and, the third with  $x=2.5$  and  $2.6$ . Rather similar spectral profiles to those of the first two groups have been reported<sup>6</sup> by Gros *et al.* in their study of various  $\text{RCo}_3\text{FeB}$  compounds, where  $R$  is Pr, Nd, or Sm. Third, the spectrum of  $\text{GdCo}_{3.80}\text{Fe}_{0.20}\text{B}$  seems to be a combination of the spectra observed for  $x=0.15$  and  $0.25$ .

X-ray diffraction characterization has indicated that all the  $\text{GdCo}_{4-x}\text{Fe}_x\text{B}$  compounds crystallize with the hexagonal  $P6/mmm$  space group as is found<sup>1</sup> for  $\text{CeCo}_4\text{B}$ . The unit-cell  $a$  axis increases linearly<sup>7</sup> between  $x=0$  and  $1.5$  and then remains constant between  $1.5$  and  $2.6$ . In contrast, the  $c$  axis remains constant between  $x=0$  and  $1.5$  and then increases between  $1.5$  and  $2.6$ . Thus the substitution of cobalt by iron induces an anisotropic expansion of the  $c$  axis of the unit cell, an expansion which is similar to that observed<sup>8,9,11</sup> in the  $\text{YCo}_{4-x}\text{Fe}_x\text{B}$  compounds. As a consequence of the combined changes in the  $a$  and  $c$  axes, the unit-cell volume increases essentially linearly with increasing  $x$ .

The structure of the  $\text{GdCo}_{4-x}\text{Fe}_x\text{B}$  compounds has five crystallographic sites, the  $1a$  and  $1b$  sites that contain gadolinium, the  $2c$  and  $6i$  sites that contain either cobalt or iron, and the  $2d$  site that contains boron. Thus the analysis of the iron-57 Mössbauer spectra of these compounds must take into account the possible partial or full occupation of either or both of the  $2c$  and  $6i$  sites by iron. In determining this occupancy it is useful to note that a recent room temperature neutron diffraction study of the  $\text{YCo}_{4-x}\text{Fe}_x\text{B}$  compounds<sup>11</sup> has indicated that iron first preferentially replaces cobalt on the  $2c$  site rather than on the  $6i$  site. Further, the analysis of the spectra of these solid solutions may require a modeling of the distribution of the iron or cobalt on the near-neighbor

environments of the  $2c$  and  $6i$  sites. A Wigner-Seitz cell analysis of the  $\text{YCo}_4\text{B}$  structure<sup>13</sup> indicates that the  $2c$  site has six  $6i$  near neighbors that may contain either cobalt and/or iron in the  $\text{GdCo}_{4-x}\text{Fe}_x\text{B}$  compounds. In addition, this analysis indicates that the  $6i$  site has two  $2c$  and four  $6i$  near neighbors that may contain either cobalt and/or iron. In some cases, as will be discussed below, these near neighbor environments have an influence on the observed Mössbauer spectra and, in these cases, a binomial distribution of iron and cobalt near neighbors for the  $2c$  and  $6i$  sites has been used in the spectral fits. However, because iron nearly fills the  $2c$  site in  $\text{GdCo}_{1.5}\text{Fe}_{2.5}\text{B}$  and  $\text{GdCo}_{1.4}\text{Fe}_{2.6}\text{B}$ , only the distribution of iron and cobalt on the  $6i$  site has to be considered for these compounds.

As has been demonstrated<sup>6</sup> by Gros *et al.*, the very different Mössbauer spectral profiles observed in Figs. 1 and 2 result from differing orientations of the magnetic moments and, hence, hyperfine fields of iron in the presence of large quadrupole interactions on the  $2c$  and the  $6i$  sites. A comparison of the earlier spectra<sup>6</sup> with the spectra shown in Figs. 1 and 2 indicates that at room temperature the  $\text{GdCo}_{4-x}\text{Fe}_x\text{B}$  compounds exhibit an axial magnetization when  $x$  is  $0.10$ ,  $0.15$ ,  $2.5$ , and  $2.6$ , whereas they exhibit a basal magnetization when  $x$  is  $0.25$ ,  $1$ , and  $2$ . These orientations are in agreement with the easy direction of the magnetization reported earlier.<sup>7</sup>

The simultaneous presence of both small hyperfine fields and large quadrupole interactions in the iron-57 Mössbauer spectra of the  $\text{GdCo}_{4-x}\text{Fe}_x\text{B}$  compounds prevents their analysis with a first-order perturbation of the Zeeman magnetic Hamiltonian by the quadrupole interaction. Spectral fits with this first-order approximation have been used earlier<sup>10</sup> to fit

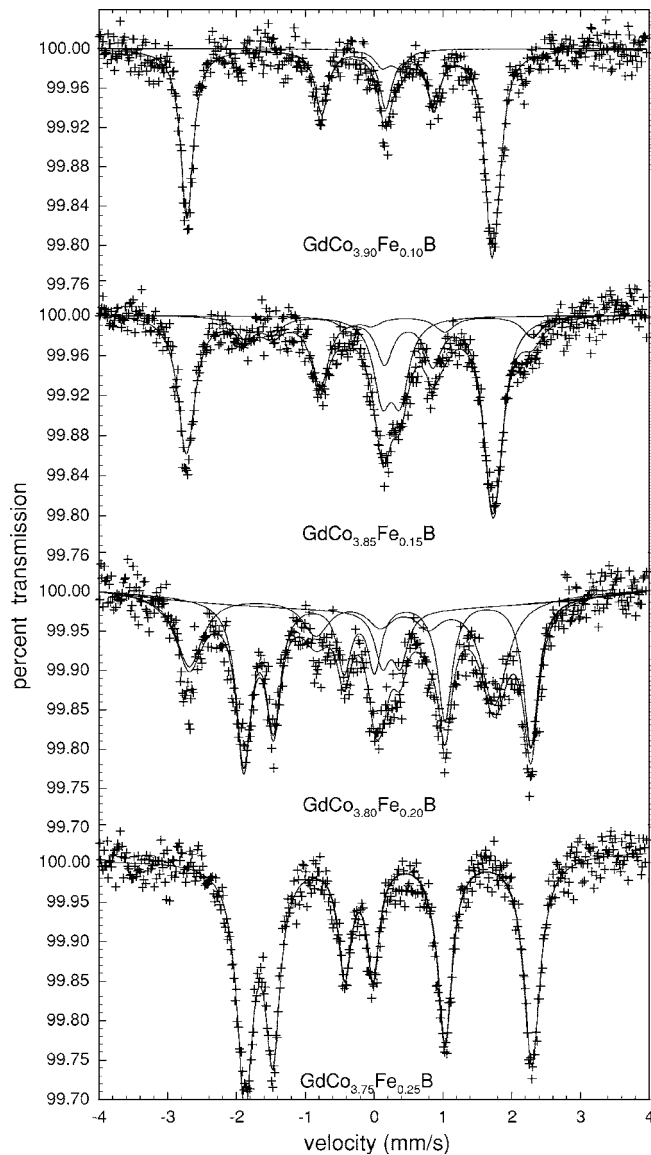


FIG. 1. The room temperature Mössbauer spectra of the  $\text{GdCo}_{4-x}\text{Fe}_x\text{B}$  compounds with  $0.10 \leq x \leq 0.25$ .

the Mössbauer spectra of  $\text{ErCo}_{4-x}\text{Fe}_x\text{B}$  and the resulting hyperfine parameters must be interpreted with great caution. Hence, the exact solution of the iron-57 excited state Hamiltonian has been used to fit the Mössbauer spectra of the  $\text{GdCo}_{4-x}\text{Fe}_x\text{B}$  compounds. The resulting fits, referred below as full Hamiltonian fits, are shown as the lines and spectral components in Figs. 1 and 2; the corresponding spectral parameters are given in Table I.

In the full Hamiltonian fits, the asymmetry parameter  $\eta$  of the 2c and 6i sites has been constrained to 0 and 1, respectively, in agreement with the point symmetry of these sites.<sup>6</sup> The Euler angles  $\theta$  and  $\phi$  of the hyperfine field in the electric field gradient axes depend on the orientation of the iron magnetic moments in the unit cell. In the case of an axial orientation of the 2c iron magnetic moments, designated here as  $2c_{\parallel}$ ,  $\theta$  is 0°, whereas in the case of a basal orientation of the moments, designated here as  $2c_{\perp}$ ,  $\theta$  and  $\phi$  are 90 and 0°, respectively. In the case of an axial orientation of the 6i iron magnetic moments,  $\theta$  and  $\phi$  are 90 and 0°,

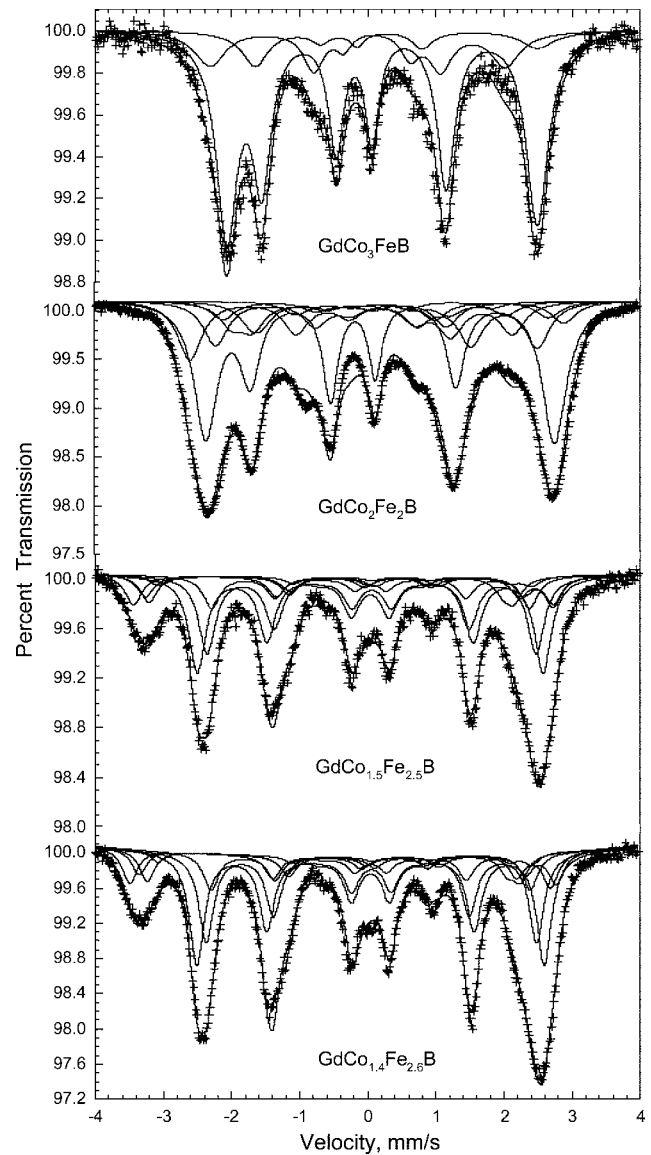


FIG. 2. The room temperature Mössbauer spectra of the  $\text{GdCo}_{4-x}\text{Fe}_x\text{B}$  compounds with  $1 \leq x \leq 2.6$ .

respectively. Furthermore, in the case of a basal orientation of the iron magnetic moments, because the principal axis of the electric field gradient  $V_{zz}$  of the 6i site is along [100], the 6i site must be subdivided into two magnetically inequivalent sites, the  $6i_1$  and  $6i_2$  subsites herein, with relative populations of one and two, respectively. In this case, the angles  $\theta$  and  $\phi$  of the hyperfine field are 0 and 90° for the  $6i_1$  subsite and 120 and 90° for the  $6i_2$  subsite, respectively. The linewidths, isomer shifts, and quadrupole interactions of the  $6i_1$  and  $6i_2$  subsites have been constrained to be the same.

In addition to adjusting the above hyperfine parameters and the linewidth, an incremental linewidth has also been fit in order to account for the distribution of cobalt and iron on the near neighbors of the 2c and 6i sites. This unitless incremental linewidth  $\Delta\Gamma$  has been defined as  $\Gamma(v) = \Gamma + (v - \delta)\Delta\Gamma$ , where  $v$  is the velocity and  $\delta$  is the isomer shift of a given spectral component. Finally, a texture parameter  $y$  has been introduced into the fits as a multiplying factor of the Clebsch-Gordan coefficient of the  $\Delta m = 0$  transitions. In the



case of a sextet this is essentially equivalent to a component area ratio of  $3:y:1:1:y:3$ , where  $y$  may vary from 0 for a hyperfine field parallel to the  $\gamma$ -ray direction to 4 for a hyperfine field perpendicular to the  $\gamma$ -ray direction.

#### IV. MÖSSBAUER SPECTRAL RESULTS

The fits obtained with the above model are all very good to excellent as is indicated by the solid lines in Figs. 1 and 2. The Mössbauer spectrum of  $\text{GdCo}_{3.90}\text{Fe}_{0.10}\text{B}$ , which is clearly indicative of axial magnetization, is well fitted with one sextet assigned to the  $2c_{\parallel}$  site. However, a doublet with 6.5% of the spectral area must be introduced into the fit to account for the spectral intensity observed at approximately 0.25 mm/s, a doublet that results from the presence of traces of iron in the beryllium of the detector window.

Initial fits of the Mössbauer spectrum of  $\text{GdCo}_{3.85}\text{Fe}_{0.15}\text{B}$  with one sextet assigned to the  $2c_{\parallel}$  site with axial magnetization were rather good, but the shoulder observed at approximately 2.2 mm/s indicates that some of the iron on the  $2c$  site experiences a basal magnetization. Subsequent fits revealed that 65% of the total iron in  $\text{GdCo}_{3.85}\text{Fe}_{0.15}\text{B}$  exhibits an axial magnetization whereas 15% has a basal magnetization. The final fit also required a doublet with 20% of the spectral area, which again presumably results, at least in part, from the presence of traces of iron in the beryllium of the detector window.

The 295 K spectrum of  $\text{GdCo}_{3.75}\text{Fe}_{0.25}\text{B}$  is well fitted with a single magnetic component in which all of the iron experiences a basal magnetization. The same basal magnetization is also observed in the Mössbauer spectra of  $\text{GdCo}_3\text{FeB}$  and  $\text{GdCo}_2\text{Fe}_2\text{B}$ . However, the spectrum of  $\text{GdCo}_3\text{FeB}$  is broadened as compared with that of  $\text{GdCo}_{3.75}\text{Fe}_{0.25}\text{B}$ , a broadening that results from the presence of some iron on the  $6i$  site, which adds two additional  $6i$  components, see the top of Fig. 2.

A comparison of the spectrum of  $\text{GdCo}_2\text{Fe}_2\text{B}$  with that of  $\text{GdCo}_3\text{FeB}$ , see the top half of Fig. 2, reveals extensive additional broadening in the former spectrum. As a consequence of this extensive broadening, it was *not* possible to obtain a reasonable fit of the spectrum of  $\text{GdCo}_2\text{Fe}_2\text{B}$  with one component for the  $2c$  site and two components for the  $6i$  site. Thus the distribution of iron and cobalt on the four  $6i$  near neighbors of the  $6i$  site must produce a significant perturbation of the hyperfine parameters of this site, a perturbation that must be included in the fitting model. In order to do this we have assumed a random distribution of iron and cobalt on the  $6i$  site, and have used and constrained the relative areas of the three components for the  $6i_1$  and  $6i_2$  sites to those derived from the binomial distribution of iron on their near-neighbor  $6i$  sites. These three components correspond to 0, 1, and 2 or more irons on the near-neighbor  $6i$  sites. The result of this fit, which uses six binomial components with no incremental linewidth for the  $6i$  site and one component with an incremental linewidth broadening for the  $2c$  site, is shown in Fig. 2. Rather surprisingly, the  $2c$  component does not exhibit extensive broadening and thus does not require a binomial distribution for its fit. This is also the case for a binomial distribution fit of the spectrum of  $\text{GdCo}_{3.75}\text{Fe}_{0.25}\text{B}$ .

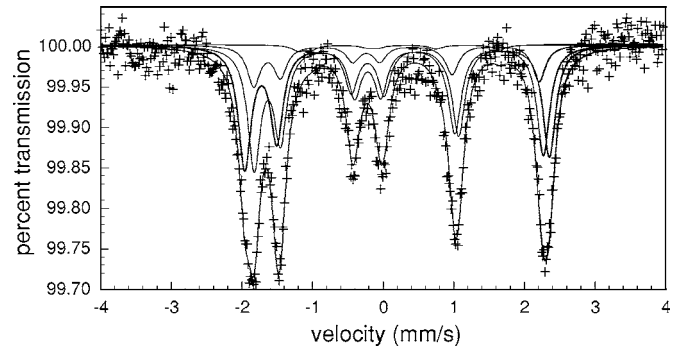


FIG. 3. The room temperature Mössbauer spectra of  $\text{GdCo}_{3.75}\text{Fe}_{0.25}\text{B}$  fit with a binomial distribution of iron on the near-neighbor  $6i$  sites.

As is shown in Fig. 3, a binomial fit of this spectrum is statistically no better than the fit with a broadened component, see Fig. 1.

As noted above, the spectra of  $\text{GdCo}_{1.5}\text{Fe}_{2.5}\text{B}$  and  $\text{GdCo}_{1.4}\text{Fe}_{2.6}\text{B}$  are again quite different from the spectra of the compounds containing less iron. This occurs because the addition of more iron has resulted in a spin reorientation, see the discussion section below, such that these high iron-content compounds exhibit axial magnetization. Indeed, their spectra would more closely resemble the spectrum of  $\text{GdCo}_{3.90}\text{Fe}_{0.10}\text{B}$ —note the presence of an absorption line at  $-2.8$  mm/s in  $\text{GdCo}_{3.90}\text{Fe}_{0.10}\text{B}$  and at  $-3.4$  mm/s in  $\text{GdCo}_{1.5}\text{Fe}_{2.5}\text{B}$  and  $\text{GdCo}_{1.4}\text{Fe}_{2.6}\text{B}$ —except that now there is a substantial occupation of the  $6i$  site by iron. Again, the absorption line at approximately  $-3.4$  mm/s, as well as the entire spectra are substantially broadened and we have been forced to fit both the  $2c$  and  $6i$  sites with a binomial distribution of iron and cobalt on their respective  $6i$  near neighbors. The resulting fits, shown in the lower half of Fig. 2, used four components for the  $2c$  sites, corresponding to 0 or 1, 2, 3, and 4 or more near-neighbor irons on the  $6i$  sites and three components for the  $6i$  sites, corresponding to 2 or less, 3, and 4 near-neighbor irons on the  $6i$  sites.

The compositional dependence of the  $2c$  and  $6i$  hyperfine fields is shown in Fig. 4(a). The hyperfine fields on both sites are relatively small between 12 and 18 T and, for both magnetic anisotropies, they increase with increasing iron content, in agreement with the increase in the average 3d magnetic moments reported earlier.<sup>7</sup> The increase in average 3d magnetic moment of approximately  $0.5\mu_B$  in going from  $x=0.2$  to 2.6 corresponds to an increase in the  $2c$  hyperfine field of 4.56 T or  $9.12\text{ T}/\mu_B$ . Furthermore, as previously observed<sup>13</sup> in the  $\text{YCo}_{4-x}\text{Fe}_x\text{B}$  compounds, where  $x$  is 1, 2, and 3, the hyperfine field on the iron  $2c$  site is larger in the case of axial magnetization. Both the relatively small values of all the hyperfine fields and the somewhat larger fields observed for the  $2c_{\parallel}$  sites as compared with the  $2c_{\perp}$  sites result from a combination of the Fermi contact and orbital contributions to the hyperfine fields, which have been discussed earlier.<sup>13</sup>

The compositional dependence of the  $2c$  and  $6i$  isomer shifts is shown in Fig. 4(b). The  $2c$  and  $6i$  isomer shifts seem to increase with increasing iron content in agreement with the increase in unit-cell volume.<sup>7</sup> The quadrupole interac-

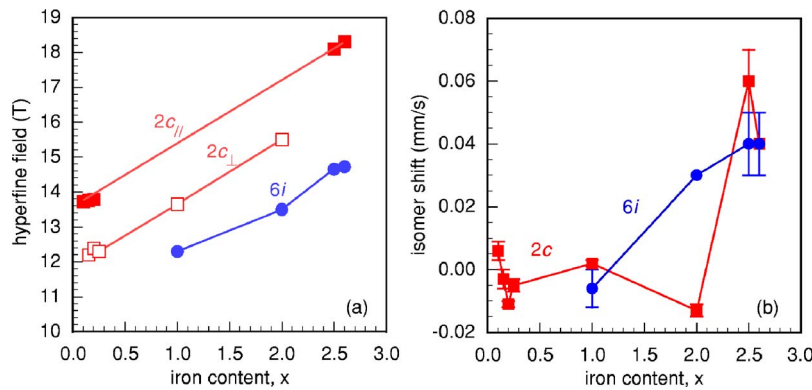


FIG. 4. (Color online) The compositional dependence of the  $2c$  and  $6i$  site hyperfine fields (a) and the isomer shifts (b) in the  $\text{GdCo}_{4-x}\text{Fe}_x\text{B}$  compounds. The error bars on the hyperfine fields are smaller than the size of the data points. This is also the case for some of the error bars on the isomer shifts.

tions of both the  $2c$  and  $6i$  sites are essentially independent of iron content. Hence, it seems that the quadrupole interactions are not sensitive to either the replacement of cobalt by iron or the concurrent expansion of the lattice.

The compositional dependence of the iron  $2c$  occupancy, determined from the relative area of the iron  $2c$  Mössbauer spectral components for the  $\text{GdCo}_{4-x}\text{Fe}_x\text{B}$  compounds, is shown in Fig. 5 together with the iron  $2c$  occupancy determined<sup>11</sup> by a neutron diffraction study of the isotypic  $\text{YCo}_{4-x}\text{Fe}_x\text{B}$  compounds. In both series, there is a strong and similar preferential occupation of the  $2c$  site by iron. The iron  $2c$  occupancy determined here from the relative area of the  $2c$  components in  $\text{GdCo}_{4-x}\text{Fe}_x\text{B}$ , with  $x=2.5$  and  $2.6$  is slightly smaller than expected from the occupancy observed in  $\text{YCoFe}_3\text{B}$ . However, the limitations imposed by using a binomial distribution fit to determine the variable iron occupancy of the  $2c$  site limits the accuracy on these two low values.

## V. DISCUSSION AND CONCLUSIONS

The Mössbauer spectra of the  $\text{GdCo}_{4-x}\text{Fe}_x\text{B}$  compounds, with  $x=0.10, 0.15, 0.20, 0.25, 1, 2, 2.5$ , and  $2.6$ , obtained at room temperature have been analyzed with a model that takes into account both the orientation of the easy magnetization direction and the distribution of iron and cobalt near neighbors of the two iron sites. Because the hyperfine fields are relatively small, between 12 and 18 T, and the quadru-

pole interactions are large at approximately  $-1.0$  and  $+0.9$  mm/s, a first-order approximation of the perturbation of the magnetic Zeeman interaction by the quadrupole interaction cannot be used and a solution of the full Hamiltonian for the iron-57 nuclear excited state must be used to fit the spectra. The hyperfine fields increase with increasing iron content. The hyperfine fields observed for an axial orientation of the magnetization are found to be larger than for a basal orientation of the magnetization. The iron  $2c$  occupancies, determined from the relative areas of the iron  $2c$  Mössbauer spectral components in the  $\text{GdCo}_{4-x}\text{Fe}_x\text{B}$  spectra, agree with those previously observed by neutron diffraction in the related  $\text{YCo}_{4-x}\text{Fe}_x\text{B}$  compounds.

The fits of the Mössbauer spectra without the inclusion of the texture parameter  $\gamma$  were substantially poorer than those shown in Figs. 1 and 2. More specifically, although the positions of the absorption lines were accurately determined, their relative intensities were often under- or overestimated. Because the  $\text{GdCo}_{4-x}\text{Fe}_x\text{B}$  compounds exhibit substantial magnetic anisotropy, it is quite likely that the absorbers exhibit at least some preferential orientation of the crystallites that leads to texture in the spectral absorbers.

The influence of the substitution of iron for cobalt on the magnetic anisotropy of the  $\text{GdCo}_{4-x}\text{Fe}_x\text{B}$  compounds with  $x \leq 0.1$ , has been previously reported.<sup>14</sup> At both 77 and 300 K, the compounds with  $x \leq 0.04$  exhibited an axial magnetic anisotropy, whereas the compounds with  $0.08 \leq x \leq 0.1$  exhibited a basal magnetic anisotropy. The intermediate compounds with  $0.05 \leq x \leq 0.07$  exhibited a spin reorientation from basal to axial magnetic anisotropy between 77 and 300 K. This behavior of the magnetic anisotropy with changing  $x$  is slightly different from that observed here. Hence, we are forced to conclude that the iron content  $x$  for which the magnetization changes from axial to basal depends upon the sample preparation.

In the earlier<sup>7</sup> report and in the work reported herein on the  $\text{GdCo}_{4-x}\text{Fe}_x\text{B}$  compounds a much wider,  $0.10 \leq x \leq 2.6$  range of iron content has been studied, a range that better reveals the role of the iron in determining the magnetic anisotropy. An individual site magnetic anisotropy model<sup>15</sup> has successfully described<sup>14</sup> the change in magnetic anisotropy for  $x \leq 1.6$ . In this model, the first-order magnetic anisotropy constant  $K_1(x)$  is given by

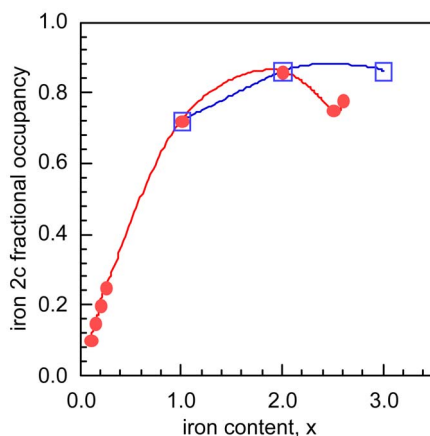


FIG. 5. (Color online) The compositional dependence of the iron  $2c$  occupancy in the  $\text{GdCo}_{4-x}\text{Fe}_x\text{B}$  compounds (circles) and in the  $\text{YCo}_{4-x}\text{Fe}_x\text{B}$  compounds (squares).

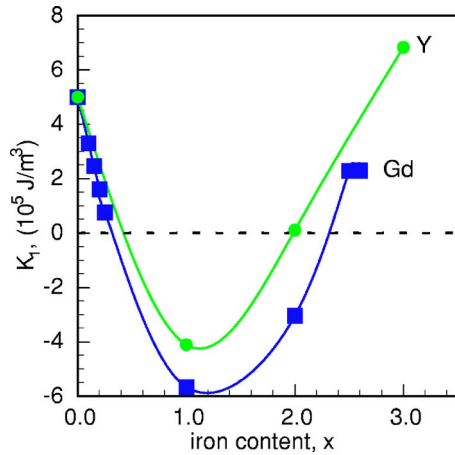


FIG. 6. (Color online) The compositional dependence of the first-order anisotropy constant in the  $\text{GdCo}_{4-x}\text{Fe}_x\text{B}$  compounds (squares) and in the  $\text{YCo}_{4-x}\text{Fe}_x\text{B}$  compounds (circles). The curves have been calculated as reported in Ref. 14.

$$K_1(x) = K_1(0) + 2f_{2c}(x)\Delta K_1^{2c} + 6f_{6i}(x)\Delta K_1^{6i}, \quad (1)$$

where  $K_1(0) = 5 \times 10^5 \text{ J/m}^3$  is the magnetic anisotropy constant for  $\text{GdCo}_4\text{B}$ ,  $f_{2c}(x)$  and  $f_{6i}(x)$  are the iron  $2c$  and  $6i$  occupancies, and  $\Delta K_1^{2c} = -8.49 \times 10^5 \text{ J/m}^3$  and  $\Delta K_1^{6i} = +2.88 \times 10^5 \text{ J/m}^3$  are the differences in the iron and cobalt contributions to the magnetic anisotropy for the  $2c$  and  $6i$  sites, respectively.

Figure 6 shows the compositional dependence of the first-order magnetic anisotropy constant calculated by using Eq. (1), the iron  $6i$  and  $2c$  occupancies, determined from the Mössbauer spectral areas, and the numerical values given above for the  $\text{GdCo}_{4-x}\text{Fe}_x\text{B}$  compounds with  $0.10 \leq x \leq 2.6$ . This figure also shows the equivalent dependence for the  $\text{YCo}_{4-x}\text{Fe}_x\text{B}$  compounds, with  $x=1, 2$ , and  $3$ , a dependence that has been calculated by using the iron  $6i$  and  $2c$  occupancies determined<sup>11,13</sup> from neutron diffraction and  $\Delta K_1^{2c} = -7.55 \times 10^5 \text{ J/m}^3$  and  $\Delta K_1^{6i} = +3.55 \times 10^5 \text{ J/m}^3$ .<sup>14</sup> In both series of compounds, a change from axial magnetic anisotropy in  $\text{GdCo}_4\text{B}$  and  $\text{YCo}_4\text{B}$  to a basal magnetic anisotropy is predicted for  $x=0.3$  and  $0.4$  in the  $\text{GdCo}_{4-x}\text{Fe}_x\text{B}$  and  $\text{YCo}_{4-x}\text{Fe}_x\text{B}$  compounds, respectively. The present study shows that for  $\text{GdCo}_{4-x}\text{Fe}_x\text{B}$  this spin reorientation actually occurs for  $0.15 < x < 0.25$ . This spin reorientation is easily understood in view of the preferential iron occupancy of the

$2c$  sites and its negative, i.e., basal, contribution to the magnetic anisotropy. Perhaps more interestingly, this model also correctly predicts a second spin reorientation from basal back to axial for  $x > 2.0$  and  $2.3$  in the  $\text{YCo}_{4-x}\text{Fe}_x\text{B}$  and  $\text{GdCo}_{4-x}\text{Fe}_x\text{B}$  compounds, respectively. Indeed, as we have shown above and elsewhere,<sup>13</sup>  $\text{GdCo}_{1.5}\text{Fe}_{2.5}\text{B}$  and  $\text{YCoFe}_3\text{B}$  exhibit axial magnetizations at room temperature. This second spin reorientation in the larger  $x$  compositional range results from the filling of the  $6i$  sites by iron and its positive, i.e., axial, contribution to the magnetic anisotropy. In conclusion, the combination of the iron Mössbauer spectral and the individual site magnetic anisotropy model provides<sup>15</sup> a much better insight into the role of the iron in determining the magnetic anisotropies of the  $\text{GdCo}_{4-x}\text{Fe}_x\text{B}$  and  $\text{YCo}_{4-x}\text{Fe}_x\text{B}$  compounds.

## ACKNOWLEDGMENTS

The authors thank Z. Lin and Professor O. Isnard for their help and suggestions during the course of this work. This work was partially supported by the Fonds National de la Recherche Scientifique, Belgium, through Grant No. 9.456595.

- <sup>1</sup>Y. B. Kuz'ma and N. S. Bilonizhko, *Sov. Phys. Crystallogr.* **18**, 447 (1974).
- <sup>2</sup>Y. B. Kuz'ma, N. S. Bilonizhko, S. I. Mykhailenko, G. F. Stepanova, and N. F. Chaban, *J. Less-Common Met.* **67**, 51 (1979).
- <sup>3</sup>N. A. El-Masry and H. H. Stadelmaier, *Z. Metallkd.* **74**, 86 (1983).
- <sup>4</sup>F. Spada, C. Abache, and H. Oesterreicher, *J. Less-Common Met.* **99**, L21 (1986).
- <sup>5</sup>S. Y. Jiang, W. E. Wallace, and E. Burzo, *J. Magn. Magn. Mater.* **61**, 257 (1986).
- <sup>6</sup>Y. Gros, F. Hartmann-Boutron, C. Meyer, M. A. Fremy, and P. Tenaud, *J. Magn. Magn. Mater.* **74**, 319 (1988).
- <sup>7</sup>Z. Drzazga, E. Popiel, and A. Winiarska, *J. Magn. Magn. Mater.* **104–107**, 1437 (1992).
- <sup>8</sup>C. Chacon and O. Isnard, *Physica B* **276–278**, 652 (2000).
- <sup>9</sup>C. Chacon, doctoral dissertation, Université Joseph Fourier—Grenoble I, 2000.
- <sup>10</sup>F. Maruyama, Y. Amako, and H. Nagai, *J. Alloys Compd.* (in press).
- <sup>11</sup>O. Chacon and O. Isnard, *J. Appl. Phys.* **89**, 71 (2001).
- <sup>12</sup>E. Burzo, V. Pop, and N. Plugaru, *J. Magn. Magn. Mater.* **97**, 147 (1991).
- <sup>13</sup>G. J. Long, R. P. Hermann, F. Grandjean, C. Chacon, and O. Isnard, *J. Phys.: Condens. Matter* **18**, 10765 (2006).
- <sup>14</sup>C. V. Thang, N. P. Thuy, J. P. Liu, N. T. Hien, and T. D. Hien, *J. Magn. Magn. Mater.* **147**, 55 (1995).
- <sup>15</sup>J. J. M. Franse, F. E. Kayzel, and N. P. Thuy, *J. Magn. Magn. Mater.* **129**, 1211 (1992).